

Generalized Nambu-Goldstone pion in dense matter: a schematic NJL model

Yifan Song and Gordon Baym¹

¹*Department of Physics, University of Illinois at Urbana-Champaign.*

(Dated: November 27, 2024)

Chiral symmetry is always broken in cold, dense matter, by chiral condensation at low densities and by diquark condensation at high density. We construct here, within a schematic Nambu-Jona-Lasinio (NJL) model, the corresponding generalized Nambu-Goldstone pion, π_G . As we show, the π_G mode naturally emerges as a linear combination of the $\langle\bar{q}q\rangle$ vacuum pion π and the $\langle qq\rangle$ diquark-condensate pion $\tilde{\pi}$, with q the quark field, and continuously evolves with increasing density from being π -like in the vacuum to $\tilde{\pi}$ -like in the high density diquark pairing phase. We calculate the density-dependent mass, decay constant, and coupling to quarks of the π_G , and derive a generalized Gell-Mann–Oakes–Renner (GMOR) relation in the presence of a finite bare quark mass m_q . We briefly discuss the implications of the results to possible Bose condensation of π_G in more realistic models.

I. INTRODUCTION

Chiral symmetry, spontaneously broken in the vacuum and in low density nuclear matter by chiral condensation – with order parameter $\langle\bar{q}q\rangle$ – gives rise to the pseudoscalar octet of Nambu-Goldstone (NG) bosons, pions, kaons, and eta. In the quark matter regime at densities well above normal nuclear matter density, BCS diquark pairing is predicted [1], either in a color-flavor-locked (CFL) phase or a partially paired phase dependent on the density and the u , d , and s quark masses; the resulting diquark condensates $\langle qq\rangle$ continue to break chiral symmetry at high density¹ [5–8], even though the chiral condensates $\langle\bar{q}q\rangle$ gradually disappear. As a result, the vacuum meson modes, corresponding to fluctuations of the $\langle\bar{q}q\rangle$ order parameter, become replaced with diquark condensate meson modes corresponding to fluctuations of the $\langle qq\rangle$ order parameter in dense quark matter [9, 10]. Between low density nuclear matter and high density quark matter, we expect an extensive coexistence region of finite $\langle\bar{q}q\rangle$ and $\langle qq\rangle$, in which the NG modes are a combination of the vacuum meson modes and diquark-condensate meson modes [11–13]. As the density increases, the chiral NG modes evolve from vacuum mesons to diquark-condensate mesons, and their physical properties such as masses, decay, and interaction with quarks are modified as the $\langle\bar{q}q\rangle$ condensates are gradually replaced by the $\langle qq\rangle$ condensates.

While chiral NG mesons have been studied in the limits of low density (non-BCS paired) $\bar{q}q$ condensed matter [14–18] and high density pure-BCS qq paired matter

[11, 19–21] using the Nambu-Jona-Lasinio (NJL) model [22–24], a quantitative description of NG mesons at intermediate densities remains an open problem. Such a description requires adopting specific models to describe the changing phase structure with increasing density, itself an unresolved issue [5]. In this paper, we study the chiral structure of a simplified single flavor, single color NJL model that includes both scalar and pseudoscalar condensates. Such a model has a single chiral NG mode, which we refer to as the *generalized pion*,² π_G , corresponding to simultaneous fluctuations of the $\langle\bar{q}q\rangle$ and $\langle qq\rangle$ order parameters. The resulting phase diagram, with properly chosen model interaction parameters, mimics the more realistic QCD phase diagram in terms of chiral symmetry breaking by the low and high density condensates, which are here connected smoothly by a coexistence region (for sophisticated NJL constructions of QCD phase diagram, see e.g., [3, 25–36]). The generalized pion continuously evolves from the vacuum pion, π , in the low density chirally broken phase to the diquark-condensate pion, $\tilde{\pi}$, in the high density BCS phase; its mass and decay constant are continuous functions of quark density, and obey a generalized Gell-Mann–Oakes–Renner (GMOR) relation, which we calculate to second order in m_q . Its coupling vertex to the quark field also changes continuously with increasing density.

The present study is a first step in understanding in detail the density-dependent properties of the pseudoscalar mesons extrapolated into high density quark matter, and is readily generalized to more realistic models with multiple flavors and colors to quantitatively study the meson mass ordering reversal problem [9]. In addition to clarifying the QCD phase diagram in terms of generalized meson condensation, the study of the π_G mode also con-

¹ Depending on the specific diquark condensation at different densities [2–4], the $SU(3)_L \otimes SU(3)_R$ chiral symmetry may only be partially broken. In the partially paired “2SC” isoscalar phase, likely favored at moderate density where only up and down quarks pair, the isospin subgroup $SU(2)_L \otimes SU(2)_R$ of the chiral symmetry remains unbroken by the 2SC diquark condensate. On the other hand, in the CFL phase at high density, all eight axial generators of the chiral symmetry are broken by the CFL diquark condensate, in which all quark flavors are paired.

² The name “generalized mesons” was used, e.g., in [12], to describe the $\bar{q}q\bar{q}q$ modes corresponding to fluctuations of the diquark condensates at high density. For clarity, we refer in this paper to the NG modes (a combination of $\bar{q}q$ and $\bar{q}q\bar{q}q$ modes) as “generalized mesons,” the $\bar{q}q\bar{q}q$ modes as “diquark-condensate mesons,” and the usual $\bar{q}q$ modes as “vacuum mesons.”

tributes to understanding the thermodynamics of dense matter, and thus eventually the interiors and cooling of neutron stars [37].

In Sec. II of this paper we introduce the model NJL Lagrangian, analytically solve it in the mean field approximation, and discuss the quasiparticle spectrum and energy eigenvectors, while in Sec. III we compute the quark propagator as well as the gap equations in the even parity, spin-singlet, or “scalar,” ground state, without pion condensation. Then, in Sec. IV we investigate the phase diagram and thermodynamic stability of the system as a function of the model chiral and diquark coupling strengths, which enables us to restrict the parameter space in terms of an ultraviolet cutoff, in order that the resulting phase diagram includes a chirally broken vacuum phase and a high density BCS phase, connected by a coexistence phase at intermediate density, thus mimicking the more realistic phase diagrams in NJL studies of cold dense matter.

We next discuss the collective modes in detail in Sec. V. We first identify all the six collective modes in the chiral limit in Sec. VA corresponding to fluctuations of the chiral and diquark order parameters $\langle \bar{q}q \rangle$ and $\langle qq \rangle$. We then focus on the two pseudoscalar pionic modes π and $\tilde{\pi}$ in particular, calculating their mixing mass matrix in Sec. VB and their decay constants in Sec. VC, relating them to the mass and decay constant of the re-diagonalized NG mode π_G , and we then derive the density-dependent coupling vertex of π_G to quarks in the medium. In Sec. VD we look at the modifications introduced by a finite bare quark mass m_q , e.g., its effect on the π_G mass. We derive the matrix generalization of the GMOR relation, deriving the two masses of the two pionic modes to second order in m_q , and discuss their behavior with varying density. Finally, in Sec. VI we briefly comment on the implications of possible condensates of the NG mode in quark matter, together with several other open questions, such as the possible roles of a new massive mode corresponding to the phase difference between scalar and pseudoscalar diquark condensates.

Throughout we assume zero temperature unless stated otherwise, and use units $\hbar = c = 1$.

II. LAGRANGIAN, GAP EQUATIONS, QUASIPARTICLE DISPERSION RELATIONS AND ENERGY EIGENSTATES

We focus on the Lagrangian,

$$\mathcal{L} = \bar{q} (i\partial - m_q + \gamma_0\mu) q + G \left[(\bar{q}q)^2 + (\bar{q}i\gamma_5 q)^2 \right] + H \left[(q^T i\gamma_5 C q) (\bar{q}i\gamma_5 C \bar{q}^T) + (q^T C q) (\bar{q}C \bar{q}^T) \right], \quad (1)$$

where q is the quark field with bare mass m_q and quark chemical potential μ ; γ^μ are Dirac gamma matrices and $\gamma^5 = i\gamma^0\gamma^1\gamma^2\gamma^3$, $C = i\gamma^0\gamma^2$ is the charge conjugate matrix, G is the coupling strength for the four-quark chiral interaction term, and H is the strength of the spin-singlet

pairing interaction; G and H are model parameters. The 4-quark interaction terms exhibit equal coupling in the scalar and pseudoscalar channels. As a result, the model for vanishing m_q has a $U(1)_L \otimes U(1)_R$ chiral symmetry³ of the quark field. Finally, as the four-fermion interaction in this model is not renormalizable, we will adopt a three-momentum cutoff Λ to regulate the momentum integrals throughout this work.

We solve this model in the mean field approximation. We define the vacuum expectation value of the composite operators,⁴

$$\sigma = 2G\langle \bar{q}q \rangle, \quad \pi = 2G\langle \bar{q}i\gamma_5 q \rangle, \\ \Delta_s = 2H\langle \bar{q}i\gamma_5 C \bar{q}^T \rangle, \quad \Delta_{ps} = 2H\langle \bar{q}C \bar{q}^T \rangle; \quad (2)$$

here Δ_s is the pairing amplitude in scalar channel, and Δ_{ps} in pseudoscalar channel. The condensates σ and π serve as the order parameters of spontaneous chiral symmetry breaking at low density; the fluctuations of σ and π around their ground state values correspond to the NG boson (the vacuum pion) and the massive Higgs-like mode. Also, under axial $U(1)_A$ rotation Δ_s and Δ_{ps} rotate into each other; thus, a non-vanishing expectation value of either of these diquark operators also indicates broken chiral symmetry. We work in the homogeneous phase, so that the mean fields are constant in space.

We use the Nambu-Gor’kov formalism, defining the charge conjugate quark field $q^C = C\bar{q}^T$, and forming the Nambu-Gor’kov spinor $\psi \equiv (q, q^C)^T/\sqrt{2}$. Keeping leading order fluctuations of the composite operators around their expectation values, we arrive at the mean field Lagrangian,

$$\mathcal{L}_{MF} = \bar{\psi} S_{MF}^{-1} \psi - \frac{\sigma^2 + \pi^2}{4G} - \frac{|\Delta_s|^2 + |\Delta_{ps}|^2}{4H}, \quad (3)$$

with the fermion inverse propagator

$$S_{MF}^{-1} = \begin{pmatrix} i\partial - \hat{M} + \gamma^0\mu & i\gamma_5\Delta_s^* + \Delta_{ps}^* \\ i\gamma_5\Delta_s + \Delta_{ps} & i\partial - \hat{M} - \gamma^0\mu \end{pmatrix}, \quad (4)$$

where the effective quark mass matrix is $\hat{M} = m_q - \sigma - i\gamma_5\pi$. The quark eigenstates are quasiparticles of momentum \mathbf{p} with dispersion relation $\omega(\mathbf{p})$, given by the solution of

$$\det S_{MF}^{-1}(\omega(\mathbf{p}), \mathbf{p}) = 0 \quad (5)$$

³ In our single flavor schematic model we call the $U(1)_L \otimes U(1)_R = U(1)_V \otimes U(1)_A$ symmetry simply the *chiral symmetry*, in contrast to realistic NJL models with $N_f > 1$, where the $SU(N_f)_L \otimes SU(N_f)_R$ symmetry is the “chiral symmetry” and $U(1)_A$ is the $U(1)$ axial symmetry.

⁴ Our definition of diquark pairing amplitude has $i\gamma_5$ between the quark fields, compared with γ_5 alone, which is often used, e.g., in [12].

in frequency-momentum space. The result is

$$\begin{aligned}\omega(\mathbf{p}) &= \pm [(m_q - \sigma)^2 + \pi^2 + \mathbf{p}^2 + \mu^2 \\ &\quad + |\Delta_s|^2 + |\Delta_{ps}|^2 \pm 2\delta(\mathbf{p})]^{\frac{1}{2}}; \\ \delta(\mathbf{p}) &\equiv \left[(|\mathbf{p}|\mu \pm \text{Im} [\Delta_s \Delta_{ps}^*])^2 \right. \\ &\quad \left. + \mu^2 ((m_q - \sigma)^2 + \pi^2) + |(m_q - \sigma)\Delta_{ps} - \pi\Delta_s|^2 \right]^{\frac{1}{2}}.\end{aligned}\quad (6)$$

The leading “ \pm ” sign in $\omega(\mathbf{p})$ is the degeneracy introduced by the Nambu-Gor’kov formalism; the second “ \pm ” sign in front of $\delta(\mathbf{p})$ corresponds to the particle-hole branches; and the last “ \pm ” sign within $\delta(\mathbf{p})$ is a splitting caused by a relative phase between Δ_s and Δ_{ps} . All three “ \pm ” signs are independent of each other, making a total of eight eigenvalues (or four physical ones, after removing the Nambu-Gor’kov degeneracy and keeping only positive $\omega(\mathbf{p})$). In the chiral limit $m_q = 0$, all four of the combinations

$$|\Delta_s|^2 + |\Delta_{ps}|^2, \text{Im} (\Delta_s \Delta_{ps}^*), \sigma^2 + \pi^2, \text{ and } |\sigma\Delta_{ps} + \pi\Delta_s|^2 \quad (7)$$

are fully invariant under $U(1)_L \otimes U(1)_R$ rotations, so that $\omega(\mathbf{p})$ is always invariant under the full symmetry group of the Lagrangian.

In terms of the different quasiparticle eigenvalues $\omega(\mathbf{p})$, the grand thermodynamic potential per unit volume $\Omega(T, \mu)$ is given by

$$\begin{aligned}\Omega &= -T \sum_{i=1}^4 \int_{\mathbf{p}} \left[\ln \left(1 + e^{-\omega_i/T} \right) + \frac{1}{2T} (\omega_i - \omega_{i0}) \right] \\ &\quad + \frac{\sigma^2 + \pi^2}{4G} + \frac{|\Delta_s|^2 + |\Delta_{ps}|^2}{4H}.\end{aligned}\quad (8)$$

We use $\int_{\mathbf{p}}$ to denote $\int d^3p/(2\pi)^3$, and the summation is over the four positive eigenvalues ω_i . The eigenvalues ω_{i0} are given by the ω_i with the mean fields set equal to zero and $\mu = 0$, and thus the free energy Ω vanishes in the vacuum with no condensates. The value of the mean fields are self-consistently determined by minimizing Ω , resulting in a total of six equations:

$$\frac{\partial \Omega}{\partial \sigma} = \frac{\partial \Omega}{\partial \pi} = \frac{\partial \Omega}{\partial \Delta_s} = \frac{\partial \Omega}{\partial \Delta_s^*} = \frac{\partial \Omega}{\partial \Delta_{ps}} = \frac{\partial \Omega}{\partial \Delta_{ps}^*} = 0, \quad (9)$$

which we simply refer to as “gap equations.” Only five are independent; they determine the two chiral fields and the two complex pairing gaps (to within an overall phase). In the chiral limit, only four of the gap equations are independent.

III. SCALAR CHIRAL AND DIQUARK CONDENSATES

Owing to the symmetries of the Lagrangian (1), the solutions to the gap equations (9) are degenerate. We

focus on the particular choice in chiral limit $m_q = 0$:

$$\sigma = -M, \quad \pi = 0, \quad \Delta_s = -i\Delta, \quad \Delta_{ps} = 0. \quad (10)$$

This “scalar state” describes an even-parity, spin-singlet ground state without pion condensation. In this state, the NG boson corresponding to chiral symmetry breaking originates from fluctuations in π and Δ_{ps} , which are pseudoscalar. There are two reasons for the choice (10): as in realistic chiral symmetry breaking in QCD, the NG boson for chiral symmetry breaking is pseudoscalar. In addition the favored diquark pairing channel in ground state at high density is likely to be scalar [1]. Therefore, we focus on the quasiparticle properties and collective modes of this particular state.

The quark inverse propagator in the scalar state takes the form

$$S_0^{-1}(\omega, \mathbf{p}) = \begin{pmatrix} \not{p} - M + \gamma_0 \mu & -\gamma_5 \Delta \\ \gamma_5 \Delta & \not{p} - M - \gamma_0 \mu \end{pmatrix}. \quad (11)$$

The effective mass M and BCS gap Δ are real. By choosing Δ_s to be purely imaginary as in Eq. (10), the eigenvectors of the Hamiltonian can be chosen to be entirely real. In the scalar state the two distinct positive eigenvalues have the familiar form:

$$\omega_{\pm}(\mathbf{p}) = \sqrt{(\epsilon_{\pm}(\mathbf{p}) - \mu)^2 + \Delta^2}, \quad \epsilon_{\pm}(\mathbf{p}) = \pm \sqrt{\mathbf{p}^2 + M^2}, \quad (12)$$

each with spin degeneracy two, giving four positive eigenvalues in total. The corresponding normalized eigenvectors are

$$\begin{aligned}\lambda_{\pm}(\omega_{\pm}(\mathbf{p}), s) &= R_{\pm}(\mathbf{p}) \begin{pmatrix} v_{\pm}(\mathbf{p})r(\mathbf{p}) \\ u_{\pm}(\mathbf{p})t(\mathbf{p}) \end{pmatrix}, \\ r(\mathbf{p}) &\equiv \begin{pmatrix} s \\ \hat{P}s \end{pmatrix}, \quad t(\mathbf{p}) \equiv \begin{pmatrix} -\hat{P}s \\ s \end{pmatrix},\end{aligned}\quad (13)$$

where $s = (1, 0)^T$ or $(0, 1)^T$ are spin-1/2 spinors, $R_{\pm}^2(\mathbf{p}) \equiv (\epsilon_{\pm}(\mathbf{p}) + M)/2\epsilon_{\pm}(\mathbf{p})$ defines the normalization constant, and $\hat{P} \equiv \boldsymbol{\sigma} \cdot \mathbf{p}/(\epsilon_{\pm}(\mathbf{p}) + M)$ is a projection operator in spinor space; and the coherence functions $v_{\pm}(\mathbf{p})$, $u_{\pm}(\mathbf{p})$ are exactly analogous to the non-relativistic BCS results:

$$\begin{aligned}v_{\pm}(\mathbf{p}) &= \sqrt{\frac{\omega_{\pm}(\mathbf{p}) + \epsilon_{\pm}(\mathbf{p}) - \mu}{2\omega_{\pm}(\mathbf{p})}}, \\ u_{\pm}(\mathbf{p}) &= \sqrt{\frac{\omega_{\pm}(\mathbf{p}) - \epsilon_{\pm}(\mathbf{p}) + \mu}{2\omega_{\pm}(\mathbf{p})}};\end{aligned}\quad (14)$$

they satisfy

$$v_{\pm}(\mathbf{p})^2 + u_{\pm}(\mathbf{p})^2 = 1; \quad v_{\pm}(\mathbf{p})u_{\pm}(\mathbf{p}) = \frac{\Delta}{2\omega_{\pm}(\mathbf{p})}. \quad (15)$$

The eigenvectors corresponding to the remaining four negative eigenvalues, coming from the charge conjugate fields, are instead

$$\tilde{\lambda}_{\pm}(-\omega_{\pm}(\mathbf{p}), s) = \begin{pmatrix} u_{\pm}(\mathbf{p})r(\mathbf{p}) \\ -v_{\pm}(\mathbf{p})t(\mathbf{p}) \end{pmatrix}, \quad (16)$$

In our notation, “+” corresponds to the particle-antihole branch, and “-” to the hole-antiparticle branch.

With these explicit eigenvalues and eigenvectors, the quark propagator can be written as

$$S_0(\omega, \mathbf{p}) = \sum_{\pm, s} \left[\lambda_{\pm}(\omega_{\pm}(\mathbf{p}), s) \lambda_{\pm}^{\dagger}(\omega_{\pm}(\mathbf{p}), s) \frac{1}{\omega - \omega_{\pm}(\mathbf{p})} + \tilde{\lambda}_{\pm}(-\omega_{\pm}(\mathbf{p}), s) \tilde{\lambda}_{\pm}^{\dagger}(-\omega_{\pm}(\mathbf{p}), s) \frac{1}{\omega + \omega_{\pm}(\mathbf{p})} \right] \gamma_0, \quad (17)$$

where all eight eigenvalues are summed over. This form is useful for computing various correlation functions. Lastly, the gap equations (9) in the scalar phase reduce to the two independent equations:

$$\frac{M}{2G} = M \sum_{\pm} \int_{\mathbf{p}} \frac{1}{\omega_{\pm}(\mathbf{p})} \left(1 \mp \frac{\mu}{\sqrt{\mathbf{p}^2 + M^2}} \right), \quad (18)$$

$$\frac{\Delta}{2H} = \Delta \sum_{\pm} \int_{\mathbf{p}} \frac{1}{\omega_{\pm}(\mathbf{p})}. \quad (19)$$

IV. PHASE DIAGRAM AND STABILITY OF THE MODEL IN THE SCALAR STATE

The structure of the phase diagram in the scalar state, which is obtained by solving the gap equations (18) and (19), depends on the choice of G , H and the cutoff Λ . In realistic NJL parameter fitting, these model parameters are partially controlled by fitting model predictions to lattice results, nuclear matter, and meson properties at low baryon density. Since our model is purely schematic and has reduced color and flavor degrees of freedom, we base our choice of G and H , in terms of Λ , on only two requirements: (1) there emerges a relatively extensive co-existence phase connecting the vacuum chiral symmetry breaking phase and high density BCS phase, in order to mimic the realistic QCD phase diagram, and (2) the system remains stable throughout the phase diagram. After discussing the ranges of G and H consistent with these requirements, we construct the phase diagram in the end of this section.

We first address constraints on G in the absence of pairing, i.e., $H = 0$, $\Delta = 0$. Then, for $M \neq 0$ Eq. (18) becomes:

$$\frac{1}{2G} = \frac{1}{\pi^2} \int_{p_F}^{\Lambda} \frac{p^2 dp}{\sqrt{M^2 + p^2}}. \quad (20)$$

The integral has an upper bound for all M . Therefore, at any given Fermi momentum p_F , there is a minimum value for G , below which the chiral condensate $\sim M$ cannot develop; the minimum value can be evaluated by taking the limit $M \rightarrow 0$ in Eq. (20) while regarding G as a function of p_F :

$$G = \frac{\pi^2}{\Lambda^2 - p_F^2}. \quad (21)$$

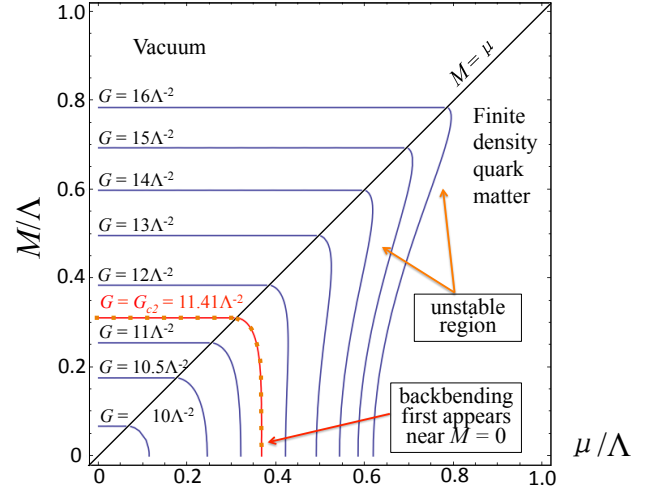


Figure 1. (Color online) Solutions to gap equation $M(\mu)$ for varying G . Backbending indicating instability first occurs at G_{c2} .

In particular, in the vacuum, $p_F = 0$, one must have $G > \pi^2/\Lambda^2$ to have a non-vanishing M . We denote this lower bound as $G_{c1} = \pi^2/\Lambda^2$.

In addition the requirement of stability under density fluctuations places an upper bound on G . Such stability requires $\partial\mu/\partial n > 0$ where $n = p_F^3/3\pi^2$ is the quark density. This condition can be related to the solution for $M(\mu)$ in Eq. (20). Differentiating $p_F(\mu)^2 = \mu^2 - M(\mu)^2$ with respect to μ we find

$$\frac{\partial n}{\partial \mu} = \frac{p_F}{\pi^2} \left(\mu - M \frac{\partial M}{\partial \mu} \right), \quad (22)$$

which must remain positive to ensure stability. From the plots of the solutions $M(\mu)$ as a family of curves given for varying G in Fig. 1, we see that above a certain value of G , the $M(\mu)$ curve begins to bend back⁵. When backbending begins with increasing G , $\partial M/\partial \mu$, at first finite and negative, becomes $-\infty$, turns to $+\infty$ and then becomes finite and positive. During backbending, Eq. (22) cannot remain positive. As a result, the system becomes unstable against density perturbations, and a homogeneous mean field solution for the scalar state is unphysical.

To compute this upper bound G_{c2} for G above which backbending of $M(\mu)$ happens, we observe that the stability is first violated, with increasing G , for $M \rightarrow 0$. In this limit, $\partial M/\partial \mu$ can be calculated by differentiating Eq. (20) with respect to μ , with the result

$$M \frac{\partial M}{\partial \mu} = \left(1 - \ln \frac{\Lambda}{p_F(\mu)} \right)^{-1} \mu. \quad (23)$$

⁵ A similar instability related to back-bending of $\langle \bar{q}q \rangle(\mu)$ also appears in lattice gauge analyses of chiral restoration, e.g., [38].

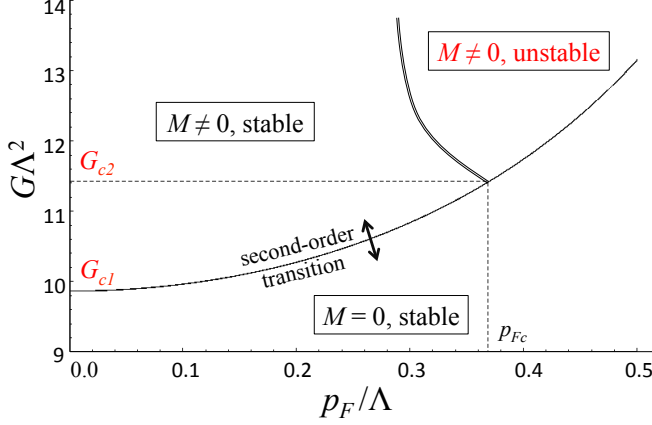


Figure 2. (Color online) Stability of the system at varying Fermi momentum p_F and G , in terms of Λ . In the range $G_{c1} < G < G_{c2}$, the system is stable with a chirally broken vacuum.

The backbending-related divergence of $\partial M/\partial \mu$ then appears at critical Fermi momentum p_{Fc} obeying $1 - \ln \Lambda/p_{Fc} = 0$, i.e., $p_{Fc} = \Lambda/e$ where e is Napier's constant. Substituting p_{Fc} back into Eq. (20) together with $M \rightarrow 0$, we find the critical value,

$$G_{c2} = \frac{\pi^2}{(1 - e^{-2})\Lambda^2}. \quad (24)$$

Finally, we plot the stability of the system at varying Fermi momentum and G in Fig. 2. In the range $G_{c1} < G < G_{c2}$, the system always undergoes a smooth second order transition from the chirally broken region $M \neq 0$ to the restored region $M = 0$.

We now turn to constraints on H . Unlike in Eq. (18) for M , the integral in Eq. (19) for Δ does not have an upper bound with varying Δ , owing to the singularity in $1/\omega_+(\mathbf{p})$ at the Fermi surface $|\mathbf{p}| = p_F$ when $\Delta \rightarrow 0$. As a result, at any density Eq. (19) always has a non-trivial solution for all H , as in non-relativistic BCS theory. Thus, diquark pairing always appears at finite densities; neither a lower nor upper bound for H is imposed by requiring diquark pairing in the model.

The requirement of emergence of a coexistence phase, however, does constrain H . For non-zero M and Δ , one can divide the gap equation (18) by M and (19) by Δ , and subtract one from the other, to find

$$\frac{1}{2H} - \frac{1}{2G} = \int_{\mathbf{p}} \frac{\mu}{\sqrt{\mathbf{p}^2 + M^2}} \left(\frac{1}{\omega_+(\mathbf{p})} - \frac{1}{\omega_-(\mathbf{p})} \right). \quad (25)$$

The right side of Eq. (25) is always positive since $\omega_+(\mathbf{p}) < \omega_-(\mathbf{p})$. As a consequence, one must have $H < G$ to have a coexistence region.

For $H \neq 0$ and $G = 0$, the system is always stable as in non-relativistic BCS. For finite G however, proving stability becomes subtle and unfortunately too algebraically

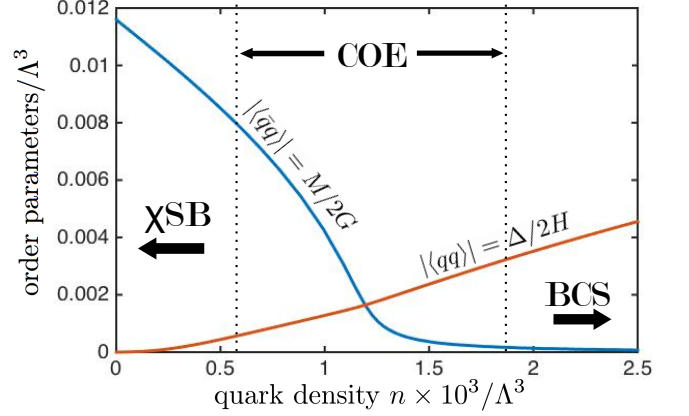


Figure 3. (Color online) The evolution of $|\langle \bar{q}q \rangle| = M/2G$ and $|\langle qq \rangle| = \Delta/2H$ against quark density n with $G = 11\Lambda^{-2}$ and $H = 6\Lambda^{-2}$. The phase diagram can be roughly divided into the chirally broken vacuum (χ SB) with $\Delta \approx 0$, $M \neq 0$, the coexistence (COE) phase where M and Δ are both finite and comparable, and the high density BCS limit where $\Delta \neq 0$ but $M \approx 0$.

overwhelming to analyze by hand. Numerical calculation suggests that instability could still develop when H becomes comparable to G , but for relatively small H , $\lesssim G/2$, a stable coexistence region can be achieved. Figure 3 shows the phase structure of the model at varying p_F plotted for a good choice $G = 11\Lambda^{-2}$ and $H = 6\Lambda^{-2}$.

In the following we discuss the collective modes of the system assuming a phase structure as in Fig. 3.

V. COLLECTIVE MODES: MASS SPECTRA AND DECAY CONSTANTS

In this section we identify the collective excitations present in the model system. The following discussion is valid for general phase between the scalar and pseudoscalar condensates, not just for the scalar state. In the chiral limit, the collective excitations include two NG modes associated with the spontaneous breakings of the $U(1)_L \otimes U(1)_R = U(1)_V \otimes U(1)_A$ symmetries – the pionic mode π_G , which is a linear combination of the vacuum pion mode π and the diquark-condensate pion mode $\tilde{\pi}$, and a phonon mode corresponding to fluctuations of the overall phase of the scalar and pseudoscalar pairing gaps, Δ_s and Δ_{ps} . In addition the system has four massive modes, one corresponding to the other linearly independent mixture of π and $\tilde{\pi}$, two Higgs-like modes corresponding to the fluctuations of the magnitudes of the chiral and diquark condensates, and finally one corresponding to the relative phase of the scalar and pseudoscalar condensates. The modes are summarized in Table I.

Mode	Description	Parity
θ_B	phonon; NG boson of broken $U(1)_V$	+
$\theta_\pi + \theta_d$	pionic mode; NG boson of broken $U(1)_A$	-
$\theta_\pi - \theta_d$	massive chiral oscillation between π and Δ_{ps}	-
M	Higgs-like; breaks $U(1)_A$	+
Δ	Higgs-like; breaks $U(1)_V$ and $U(1)_A$	+
ϕ	relative phase oscillation between Δ_s and Δ_{ps}	+

Table I. Six normal collective modes of the system.

A. General parametrization of the collective modes

The collective modes in the model system can be directly obtained via the variation of Ω under small fluctuations of the mean fields. To parametrize the modes, we write the mean fields in terms of the chiral sector axial $U(1)_A$ angle θ_π , the diquark sector $U(1)_A$ angle θ_d , the relative phase angle ϕ between Δ_s and Δ_{ps} , and the overall $U(1)_V$ phase angle θ_B :

$$\begin{aligned}\sigma &= -M \cos \theta_\pi, \\ \pi &= -M \sin \theta_\pi, \\ \Delta_s &= -i\Delta e^{i\theta_B} e^{i\phi/2} \cos \theta_d, \\ \Delta_{ps} &= i\Delta e^{i\theta_B} e^{-i\phi/2} \sin \theta_d.\end{aligned}\quad (26)$$

The oscillations of θ_π correspond to the usual pion mode, π , while those of θ_d correspond to the diquark-condensate pion, $\tilde{\pi}$. We choose $\Delta > 0$, $M > 0$, and thus $\sigma < 0$ at $\theta_\pi = 0$ (see Sec. V D). The $U(1)_V$ transformation is trivial, with both Δ_s and Δ_{ps} picking up the same phase $\theta_B \rightarrow \theta_B + \theta_V$. On the other hand, when rotating the system by a $U(1)_A$ angle θ_A , the σ and π fields transform as

$$\left. \begin{aligned}\sigma &\rightarrow \sigma \cos \theta_A - \pi \sin \theta_A \\ \pi &\rightarrow \pi \cos \theta_A + \sigma \sin \theta_A\end{aligned} \right\} \Rightarrow \theta_\pi \rightarrow \theta_\pi + \theta_A. \quad (27)$$

However the transformation of Δ_s and Δ_{ps} is more complicated:

$$\begin{aligned}\Delta_s &\rightarrow \Delta_s \cos \theta_A + \Delta_{ps} \sin \theta_A \\ &= -i\Delta \left[\cos \frac{\phi}{2} \cos (\theta_d + \theta_A) + i \sin \frac{\phi}{2} \sin (\theta_d - \theta_A) \right] \\ &\equiv -i\Delta e^{i\phi'/2} \cos \theta'_d, \\ \Delta_{ps} &\rightarrow \Delta_{ps} \cos \theta_A - \Delta_s \sin \theta_A \\ &= -i\Delta \left[-\cos \frac{\phi}{2} \sin (\theta_d + \theta_A) + i \sin \frac{\phi}{2} \sin (\theta_d - \theta_A) \right] \\ &= i\Delta e^{-i\phi'/2} \sin \theta'_d,\end{aligned}\quad (28)$$

that is, both the relative phase ϕ and the chiral angle θ_d change under the chiral transformation. When the two condensates are in phase, i.e., $\phi = 0$, the result reduces to $\theta_d \rightarrow \theta_d + \theta_A$ and $\theta_\pi \rightarrow \theta_\pi + \theta_A$. In this case,

the diquark-condensate pion corresponds to oscillations of the product of the two diquark terms, $\Delta_s \Delta_{ps}^*$. For non-zero ϕ , we have

$$\begin{aligned}\cos \theta_d &\rightarrow \cos \theta'_d = \left[\cos^2 \frac{\phi}{2} \cos^2 (\theta_d + \theta_A) \right. \\ &\quad \left. + \sin^2 \frac{\phi}{2} \sin^2 (\theta_d - \theta_A) \right]^{\frac{1}{2}}, \\ \phi &\rightarrow \phi' = 2 \tan^{-1} \left[\frac{\tan(\phi/2) \sin (\theta_d - \theta_A)}{\cos (\theta_d + \theta_A)} \right].\end{aligned}\quad (29)$$

In terms of the parametrization (26), the four invariants (7) become

$$\begin{aligned}\sigma^2 + \pi^2 &= M^2, \\ |\Delta_s|^2 + |\Delta_{ps}|^2 &= \Delta^2, \\ \text{Im} [\Delta_s \Delta_{ps}^*] &= \frac{\Delta^2}{2} \sin 2\theta_d \sin \phi,\end{aligned}\quad (30)$$

and

$$\begin{aligned}|\sigma \Delta_{ps} + \pi \Delta_s|^2 \\ = M^2 \Delta^2 \left[\sin^2 (\theta_\pi - \theta_d) - 2 \sin \theta_\pi \sin \theta_d \sin^2 \frac{\phi}{2} \right].\end{aligned}\quad (31)$$

From the six independent real degrees of freedom, $M, \Delta, \theta_\pi, \theta_d, \theta_B, \phi$, we identify the six independent normal modes:

1) The massless phonon mode, corresponding to fluctuations of θ_B . This mode is massless since the free energy does not depend on this angle.

2) The massless pionic mode, π_G , identified with fluctuations of the angle $\theta_G \equiv (\theta_\pi + \theta_d)/2$. Again the free energy does not depend on θ_G . This mode describes the simultaneous chiral rotation of σ and Δ_s in the same direction and is the NG mode.

3) A massive pionic mode, denoted as π_M , identified with fluctuations of $\theta_M \equiv (\theta_\pi - \theta_d)/2$. This mode does not correspond to a $U(1)_A$ rotation of the system and is thus always massive. The stiffness term for this mode is

$$\begin{aligned}\frac{\partial \Omega}{\partial \sin^2 (\theta_\pi - \theta_d)} &= - \sum_{\pm} \int_{\mathbf{p}} \frac{M^2 \Delta^2}{\pm \delta(\mathbf{p}) \omega_{\pm}} \\ &= \int_{\mathbf{p}} \frac{M^2 \Delta^2}{\mu \sqrt{\mathbf{p}^2 + M^2}} \left(\frac{1}{\omega_+} - \frac{1}{\omega_-} \right),\end{aligned}\quad (32)$$

which is always positive in the coexistence phase, where $M^2 \Delta^2 \neq 0$. The squared mass of the massive mode, proportional to the stiffness term, $\sim M^2 \Delta^2$, indicates that the mixing naturally occurs as long as there is a coexistence phase, even without any explicit $\bar{q}q$ - qq coupling interactions at mean field level in the Lagrangian. This massive excitation always accompanies the chiral NG mode π_G ; however it becomes unstable against decay into π_G when higher order fluctuations of the fields are taken into account. The mixing of the π and $\tilde{\pi}$ modes to form the massless π_G and the massive π_M modes is

a concrete example of the mechanism described in [12]. Here mixing results from the term $|\sigma\Delta_{ps} + \pi\Delta_s|^2$, which leads to terms $\sim \pi\tilde{\pi}$.

4) The two massive modes corresponding to fluctuations of Δ and M . These modes can be associated with oscillations in the radial direction of ‘Mexican hat’ potentials describing the broken symmetry state. In particular, the fluctuations of M are related to the heavy σ -meson in nuclear matter.

5) The massive mode associated with fluctuations of the relative phase ϕ . This mode is generally not discussed in NJL investigations of the phase diagram. If one starts in the scalar state with $\phi = 0$, a axial rotation θ_A will leave this angle untouched, as seen from Eq. (29). Note that if either Δ_s or Δ_{ps} vanishes, this mode is not present.

Having delineated the modes, we study in detail the transition from the vacuum pion mode π associated with θ_π to the diquark pion mode $\tilde{\pi}$ in BCS phase at high density associated with θ_d . We consider the fluctuations of the system about the scalar state fixing $\phi = 0$, and neglect the phonon mode as well as the massive modes M and Δ ; the latter of positive parity do not mix with the pionic modes.

B. The mass matrix for π and $\tilde{\pi}$

We first calculate the two-by-two mass matrix Σ relating the π and $\tilde{\pi}$ modes in an effective Lagrangian. To do so we expand the free energy Ω in terms of θ_π and θ_d to second order. As discussed earlier, of the two new linearly independent modes, π_G and π_M , the NG mode π_G remains massless while π_M must be massive. In fact, Eq. (32) shows that

$$\begin{aligned}\Omega &= \Omega_0 + \frac{1}{2}\theta_M^2 \int_p \sum_{\pm} \frac{1}{\omega_{\pm}(\mathbf{p})\epsilon_{\pm}(\mathbf{p})\mu} + \dots \\ &\equiv \Omega_0 + \frac{1}{2}\vec{\theta}^T \Xi \vec{\theta} + \dots\end{aligned}\quad (33)$$

where the vector $\vec{\theta} \equiv (\theta_\pi, \theta_d)^T$, and $\Omega_0 = \Omega(\theta_\pi = \theta_d = 0)$. Equation (33) immediately indicates that the stiffness matrix for the angles $\vec{\theta}$ is

$$\Xi = M^2\Delta^2a \begin{pmatrix} 1 & -1 \\ -1 & 1 \end{pmatrix}; \quad (34)$$

where

$$a(\mu) \equiv \int_p \sum_{\pm} \frac{1}{\omega_{\pm}(\mathbf{p})\epsilon_{\pm}(\mathbf{p})\mu}, \quad (35)$$

which is always positive. The matrix Ξ is related to the mass matrix Σ for the two pionic fields, i.e., the vacuum pion $\pi = f_\pi\theta_\pi$ and the diquark-condensate pion $\tilde{\pi} = f_{\tilde{\pi}}\theta_d$

(f_π and $f_{\tilde{\pi}}$ being their decay constants), by

$$\Sigma = \mathcal{F}^{-1}\Xi\mathcal{F}^{-1} = M^2\Delta^2a \begin{pmatrix} 1/f_\pi^2 & -1/f_\pi f_{\tilde{\pi}} \\ -1/f_\pi f_{\tilde{\pi}} & 1/f_{\tilde{\pi}}^2 \end{pmatrix}, \quad (36)$$

where $\mathcal{F} = \text{diag}(f_\pi, f_{\tilde{\pi}})$ is a simple invertible matrix relating π and $\tilde{\pi}$ to θ_π and θ_d :

$$\begin{pmatrix} \pi \\ \tilde{\pi} \end{pmatrix} \equiv \begin{pmatrix} \pi \\ \tilde{\pi} \end{pmatrix} = \mathcal{F} \begin{pmatrix} \theta_\pi \\ \theta_d \end{pmatrix}. \quad (37)$$

The mass matrix Σ in Eq. (36) is diagonalized by the transformation

$$\begin{pmatrix} \pi \\ \tilde{\pi} \end{pmatrix} = \frac{1}{\sqrt{f_\pi^2 + f_{\tilde{\pi}}^2}} \begin{pmatrix} f_\pi & f_{\tilde{\pi}} \\ f_{\tilde{\pi}} & -f_\pi \end{pmatrix} \begin{pmatrix} \pi_G \\ \pi_M \end{pmatrix}, \quad (38)$$

directly relating the π_G and π_M modes to the initial π and $\tilde{\pi}$ modes, with the expected mixing ratio described in Ref. [12]. The two eigenvalues of Σ , $m_G^2 = 0$ and $m_M^2 = M^2\Delta^2a(f_\pi^{-2} + f_{\tilde{\pi}}^{-2})$, give the masses of π_G and π_M .

The off-diagonal terms in Σ , corresponding to mixing of the π and $\tilde{\pi}$ modes, can also be understood in terms of perturbing the correlation functions in the chiral and diquark channel. Essentially, the corresponding off-diagonal term in Ξ can be written as

$$\begin{aligned}\Xi_{12} &= \frac{\partial}{\partial\theta_d} \left(\frac{\partial\Omega}{\partial\theta_\pi} \right) = -iM \frac{\partial\langle\bar{\psi}\Gamma_\pi\psi\rangle}{\partial\theta_d} \\ &= M\Delta \frac{\partial\langle\bar{\psi}\Gamma_\pi\psi\rangle}{\partial\langle\bar{\psi}\Gamma_{\Delta_{ps}}\psi\rangle} \sim \frac{\partial\langle\bar{q}i\gamma_5 q\rangle}{\partial\langle qq\rangle} \Big|_{\theta_\pi},\end{aligned}\quad (39)$$

where we have defined the matrices in Nambu-Gor’kov-Dirac space

$$\begin{aligned}\Gamma_\pi &\equiv \frac{1}{M} \frac{\partial S^{-1}}{\partial\theta_\pi} = \begin{pmatrix} i\gamma_5 & 0 \\ 0 & i\gamma_5 \end{pmatrix}, \\ \Gamma_{\Delta_{ps}} &\equiv \frac{1}{i\Delta} \frac{\partial S^{-1}}{\partial\theta_d} = \begin{pmatrix} 0 & 0 \\ \mathbb{1} & 0 \end{pmatrix},\end{aligned}\quad (40)$$

with $\mathbb{1}$ the 4×4 identity matrix in Dirac space.

It is instructive to compare the results (34) and (36) with the general discussion in [12], where the pion mass matrix for π and $\tilde{\pi}$ was constructed from a general Ginzburg-Landau expansion of the free energy based on symmetry principles. Up to fourth order terms in the mean fields, we see that the existence of the mixing terms, i.e., the off-diagonal terms in Σ , $\sim M^2\Delta^2$ falls naturally out of the present expansion of the free energy. The existence of these terms can be understood as a consequence of Goldstone’s theorem, since only the NG boson mode should remain massless; individual fluctuations of θ_π and θ_d no longer correspond to a global $U(1)_A$ transformation of the system, thus they cannot remain massless in the coexistence phase. Only the re-diagonalized mode π_G corresponding to the simultaneous rotation of θ_π and θ_d is massless, i.e., the mode $\theta_G = (\theta_\pi + \theta_d)/2$.

C. The decay constant of the chiral NG mode π_G

Having identified the mass matrix, we next study the decay constant of the NG mode π_G , which can be identified as the kinetic energy coefficient of θ_G in the effective Lagrangian of the bosonic fields in the long wavelength limit. To do so, we consider spatially dependent fluctuations of θ_π and θ_d . We first apply a Hubbard-Stratonovich transformation of the original quark system into a coupled system of quark fields and bosonic fields corresponding to the fluctuations of all the mean fields σ , π , Δ_s , and Δ_{ps} . We denote these fluctuations by $\hat{\sigma}$, $\hat{\pi}$, $\hat{\Delta}_s$, and $\hat{\Delta}_{ps}$, where the hat distinguishes the bosonic field fluctuations from their corresponding mean field values.

The partition function can be computed from the functional path integral:

$$\mathcal{Z} = \int d\bar{q} d\bar{q} d\hat{\sigma} d\hat{\pi} d\hat{\Delta}_s d\hat{\Delta}_s^* d\hat{\Delta}_{ps} d\hat{\Delta}_{ps}^* \times \exp \left\{ i \int d^4x \left[\bar{q} S^{-1} q - V(\hat{\sigma}, \hat{\pi}, \hat{\Delta}_s, \hat{\Delta}_{ps}) \right] \right\}, \quad (41)$$

where $t = i\tau$, with $0 \leq \tau \leq \beta$, β being the inverse temperature. The inverse quark propagator S^{-1} is perturbed from that in the scalar state S_0^{-1} , defined in Eq. (11), by the bosonic fields:

$$S^{-1} = S_0^{-1} + \hat{x}, \quad (42)$$

where

$$\hat{x} = \begin{pmatrix} \hat{\sigma} + i\gamma_5 \hat{\pi} & i\gamma_5 \hat{\Delta}_s^* + \hat{\Delta}_{ps}^* \\ i\gamma_5 \hat{\Delta}_s + \hat{\Delta}_{ps} & \hat{\sigma} + i\gamma_5 \hat{\pi} \end{pmatrix}. \quad (43)$$

The potential term is

$$V(\hat{\sigma}, \hat{\pi}, \hat{\Delta}_s, \hat{\Delta}_{ps}) = \frac{1}{4G} \left[(\hat{\sigma} - M)^2 + \hat{\pi}^2 \right] + \frac{1}{4H} \left[|\hat{\Delta}_s - i\Delta|^2 + |\hat{\Delta}_{ps}|^2 \right]. \quad (44)$$

Integrating out the quark fields to obtain the determinant of S^{-1} , and then re-exponentiating we find the effective action \mathcal{A} involving only the bosonic fields:

$$\begin{aligned} \mathcal{A} &= -i\text{Tr} \ln S^{-1} + \int d^4x V \\ &= -i\text{Tr} \ln S_0^{-1} - i\text{Tr} \left[S_0 \hat{x} - \frac{(S_0 \hat{x})^2}{2} \right] + \int d^4x V + \dots, \end{aligned} \quad (45)$$

where “Tr” denotes the sum over all indices, including position (or equivalently, momentum). In the following we drop the constant term $-i\text{Tr} \ln S_0^{-1}$ as it does not involve the bosonic fluctuations. We write the bosonic field fluctuations in terms of the spatially dependent real

bosonic fields $\hat{\theta}_\pi$ and $\hat{\theta}_d$, as in Eq. (26):

$$\begin{aligned} -M \cos \hat{\theta}_\pi &= \hat{\sigma} - M, \\ -M \sin \hat{\theta}_\pi &= \hat{\pi}, \\ -i\Delta \cos \hat{\theta}_d &= \hat{\Delta}_s - i\Delta, \\ i\Delta \sin \hat{\theta}_d &= \hat{\Delta}_{ps}. \end{aligned} \quad (46)$$

As a result, to leading order in $\hat{\theta}_\pi$ and $\hat{\theta}_d$,

$$\hat{\sigma} \approx \frac{1}{2} M \hat{\theta}_\pi^2, \quad \hat{\pi} \approx -M \hat{\theta}_\pi, \quad \hat{\Delta}_s \approx \frac{i}{2} \Delta \hat{\theta}_d^2, \quad \hat{\Delta}_{ps} \approx i\Delta \hat{\theta}_d; \quad (47)$$

using this equation we expand \mathcal{A} up to second order in $\hat{\theta}_\pi$ and $\hat{\theta}_d$, writing first,

$$\begin{aligned} \hat{x} &\approx M \begin{pmatrix} \frac{1}{2} \hat{\theta}_\pi^2 - i\gamma_5 \hat{\theta}_\pi & 0 \\ 0 & \frac{1}{2} \hat{\theta}_\pi^2 - i\gamma_5 \hat{\theta}_\pi \end{pmatrix} \\ &\quad + \Delta \begin{pmatrix} 0 & \frac{1}{2} \gamma_5 \hat{\theta}_d^2 - i\hat{\theta}_d \\ -\frac{1}{2} \gamma_5 \hat{\theta}_d^2 + i\hat{\theta}_d & 0 \end{pmatrix} \\ &\equiv M \left(\frac{1}{2} \hat{\theta}_\pi^2 \Gamma_\sigma - \hat{\theta}_\pi \Gamma_\pi \right) + \Delta \left(\frac{1}{2} \hat{\theta}_d^2 \Gamma_{\tilde{\sigma}} - \hat{\theta}_d \Gamma_{\tilde{\pi}} \right), \end{aligned} \quad (48)$$

where the matrices Γ_σ , $\Gamma_{\tilde{\sigma}}$, and $\Gamma_{\tilde{\pi}}$ in Nambu-Gor'kov-Dirac space are

$$\begin{aligned} \Gamma_\sigma &= \begin{pmatrix} \mathbb{1} & 0 \\ 0 & \mathbb{1} \end{pmatrix}, \quad \Gamma_{\tilde{\sigma}} = \begin{pmatrix} 0 & \gamma_5 \\ -\gamma_5 & 0 \end{pmatrix}, \\ \Gamma_{\tilde{\pi}} &= \begin{pmatrix} 0 & i\mathbb{1} \\ -i\mathbb{1} & 0 \end{pmatrix}, \end{aligned} \quad (49)$$

while Γ_π is already defined in Eq. (40).

In terms of real vector field $\vec{\theta} \equiv (\hat{\theta}_\pi, \hat{\theta}_d)^T$, the quadratic effective action becomes

$$\mathcal{A} \approx \frac{1}{2} \beta \mathcal{V} \int \frac{d^4k}{(2\pi)^4} \vec{\theta}(-k)^T \mathcal{D}_\theta^{-1}(k) \vec{\theta}(k), \quad (50)$$

where

$$\begin{aligned} \mathcal{D}_\theta^{-1}(k) &= \begin{pmatrix} M^2 (B_{\pi\pi}(k) - 1/2G) & M\Delta B_{\pi d}(k) \\ M\Delta B_{\pi d}(k) & \Delta^2 (B_{dd}(k) - 1/2H) \end{pmatrix} \end{aligned} \quad (51)$$

is a two-by-two matrix, and \mathcal{V} is the spatial volume of

the system. The bubbles are defined by⁶

$$\begin{aligned} B_{\pi\pi}(k) &= i \int \frac{d^4 p}{(2\pi)^4} \text{tr} (S_0(p) \Gamma_\pi S_0(p-k) \Gamma_\pi), \\ B_{\pi d}(k) &= i \int \frac{d^4 p}{(2\pi)^4} \text{tr} (S_0(p) \Gamma_\pi S_0(p-k) \Gamma_{\bar{\pi}}), \\ B_{dd}(k) &= i \int \frac{d^4 p}{(2\pi)^4} \text{tr} (S_0(p) \Gamma_{\bar{\pi}} S_0(p-k) \Gamma_{\bar{\pi}}), \end{aligned} \quad (52)$$

where “tr” denotes the Dirac and Nambu-Gor’kov trace. The factors $1/2G$ and $1/2H$ result from using the gap equations (18) and (19). Note that by the definition (50), $\mathcal{D}_\theta^{-1}(0)$ simply reduces to $-\Xi$ at zero momentum $k=0$.

At finite density, \mathcal{D}_θ^{-1} is generally not a function of the Lorentz scalar k^2 .⁷ Thus the temporal and spatial decay constants need not be equal at finite density. To second order in k ,

$$\mathcal{D}_\theta^{-1}(k) \approx -\Xi + \mathcal{Q}k_0^2 - \mathcal{Q}_v \mathbf{k}^2, \quad (53)$$

where \mathcal{Q} and \mathcal{Q}_v are also two-by-two matrices. The dispersion relations of the modes are given by the eigenvalues of \mathcal{D}_θ^{-1} , the decay constants are contained in the matrix \mathcal{Q} , and the mode velocities are included in \mathcal{Q}_v . As we show shortly, after keeping only the leading order logarithm divergencies, \mathcal{Q} is related to the matrix \mathcal{F} as defined in Eq. (37) by $\mathcal{Q} = \mathcal{F}^2$, while $\mathcal{Q}_v = \text{diag}(v_\pi^2, v_{\bar{\pi}}^2) \mathcal{Q}$ (see Eq. (60)) where v_π and $v_{\bar{\pi}}$ are the mode velocities of π and $\bar{\pi}$.

The bubbles (52) can be directly calculated from Eq. (17). To calculate the decay constant matrix \mathcal{Q} , we choose $k = (k_0, \mathbf{0})$, and then take derivatives of the bubbles with regard to k_0 . The p_0 integrals are Matsubara frequency summations with $p_0 \rightarrow i\omega_\nu = 2\pi i T \nu$ and $\int dp_0 \rightarrow 2\pi i T \sum_\nu$, where $\nu = \pm 1/2, \pm 3/2, \dots$. In terms of the quasiparticle spectrum ω_\pm , the free particle dispersion ϵ_\pm , and the coherence functions v_\pm and u_\pm defined in Sec. III – all functions of the three-momentum integration variable \mathbf{p} – the bubbles are:

$$\begin{aligned} B_{\pi\pi}(k_0^2) &= \int_{\mathbf{p}} \sum_{j,\ell=\pm} (u_j v_\ell - v_j u_\ell)^2 \left(1 - \frac{M^2 + \mathbf{p}^2}{\epsilon_j \epsilon_\ell} \right) A_{j\ell}(k_0), \\ B_{dd}(k_0^2) &= \int_{\mathbf{p}} \sum_{j,\ell=\pm} (v_j v_\ell + u_j u_\ell)^2 \left(1 - \frac{M^2 - \mathbf{p}^2}{\epsilon_j \epsilon_\ell} \right) A_{j\ell}(k_0), \\ B_{\pi d}(k_0^2) &= \int_{\mathbf{p}} \sum_{j,\ell=\pm} (v_j v_\ell + u_j u_\ell)(v_j u_\ell - u_j v_\ell) \\ &\quad \times \frac{M(\epsilon_\ell - \epsilon_j)}{\epsilon_\ell \epsilon_j} A_{j\ell}(k_0), \end{aligned} \quad (54)$$

where

$$A_{j\ell}(k_0) = \frac{1}{2} \left(-\frac{1}{k_0 - \omega_j - \omega_\ell} + \frac{1}{k_0 + \omega_j + \omega_\ell} \right). \quad (55)$$

The physical interpretation of Eqs. (54) for the bubbles is the following. The first factor, sums of products between coherence functions, indicates whether the quark loop connects the quark field with the quark field or with the charge-conjugate quark field. The second factor, involving ϵ ’s, M^2 and \mathbf{p}^2 , depends on whether the quark loop connects particle-antihole states with particle-antihole states, or with antiparticle-hole states. Both the first and second factors are at most of order unity. The final factor $A_{j\ell}$, Eq. (55), reveals the pole structure of the external frequency k_0 ; it contains a pair of poles located at $\pm(\omega_j + \omega_\ell)$ with opposite signs for the corresponding residues, representing the pion state and anti-pion state described by the bubble. In our model the pion is only neutral, thus they represent the same pion state. In $N_f = 2$ models where charged pions are present, the dual poles would represent the π^+ and the π^- state separately.

For example, consider the $B_{\pi\pi}$ bubble; the factor $(u_j v_\ell - v_j u_\ell)^2$ involves products between v and u , indicating that the quark loop connects the quark field with the charge-conjugate field; the factor $1 - (M^2 + \mathbf{p}^2)/\epsilon_j \epsilon_\ell$ vanishes unless $j = -\ell$, indicating that the particle-antihole state is connected to the antiparticle-hole state. Altogether, the quark field particle-anti-hole state is connected to the charge-conjugate antiparticle-hole state (or equivalently, to the quark field particle-antihole state itself), and the quark field antiparticle-hole state is connected to the charge-conjugate particle-antihole state (or equivalently, to the quark antiparticle-hole state).

Furthermore, the mixing bubble $\Pi_{\pi d}$ can be further simplified by using the properties, Eq. (15), of the coherence functions; we find

$$B_{\pi d}(k_0^2) = -M\Delta \int_{\mathbf{p}} \sum_{j,\ell=\pm} \frac{(\epsilon_j - \epsilon_\ell)^2}{2\epsilon_j \epsilon_\ell \omega_j \omega_\ell} A_{j\ell}(k_0). \quad (56)$$

This bubble, connecting the chiral pion mode and di-quark mode, is non-vanishing only in the coexistence region $M \neq 0$ and $\Delta \neq 0$. The bubbles are summarized diagrammatically in Fig. 4.

In terms of the bubbles, the matrix Ξ is given by $-\mathcal{D}_\theta^{-1}(k=0)$, as in Eq. (51). We find explicitly,

$$\begin{aligned} M^2 \left(B_{\pi\pi}(0) - \frac{1}{2G} \right) &= \Delta^2 \left(B_{dd}(0) - \frac{1}{2H} \right) \\ &= -M\Delta B_{\pi d}(0) = -M^2 \Delta^2 a, \end{aligned} \quad (57)$$

(a is given by Eq. (35)) confirming the expected form (34) of Ξ .

⁶ Note that with the u, d quarks replaced by protons and neutrons the bubble $B_{\pi\pi}$ is simply the self-energy of the conventional in-nuclear medium pion Green’s function.

⁷ Even in the vacuum use of a three-momentum cutoff violates Lorentz invariance.

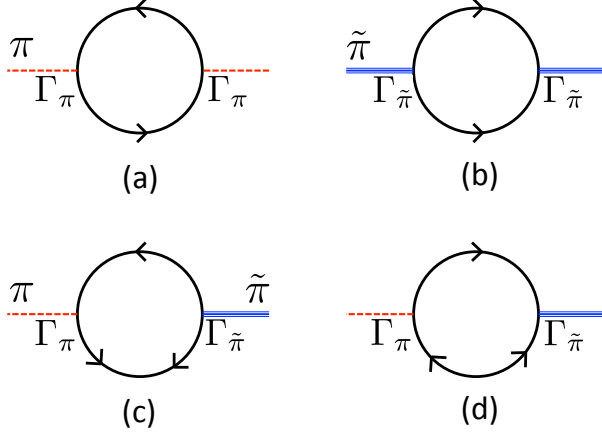


Figure 4. (Color online) Characteristic diagrams corresponding to the bubbles (54). The direct (a) π - π and (b) $\tilde{\pi}$ - $\tilde{\pi}$ bubbles correspond to $B_{\pi\pi}$ and B_{dd} , while the π - $\tilde{\pi}$ mixing bubbles such as (c) and (d) correspond to $B_{\pi d}$. Due to the breaking of $U(1)_V$ by diquark pairing, quark number is not conserved.

From Eq. (54) we calculate the \mathcal{Q} matrix:

$$\begin{aligned} \mathcal{Q}_{11} &= M^2 \int_{\mathbf{p}} \sum_{j,\ell=\pm} (u_j v_\ell - v_j u_\ell)^2 \left(1 - \frac{M^2 + \mathbf{p}^2}{\epsilon_j \epsilon_\ell} \right) W_{j\ell}, \\ \mathcal{Q}_{22} &= \Delta^2 \int_{\mathbf{p}} \sum_{j,\ell=\pm} (v_j v_\ell + u_j u_\ell)^2 \left(1 - \frac{M^2 - \mathbf{p}^2}{\epsilon_j \epsilon_\ell} \right) W_{j\ell}, \\ \mathcal{Q}_{12} &= -2M^2 \Delta^2 \int_{\mathbf{p}} \frac{1}{\omega_+ \omega_- (\omega_+ + \omega_-)^3} = \mathcal{Q}_{21}, \end{aligned} \quad (58)$$

where

$$W_{j\ell}(\mathbf{p}) \equiv \frac{1}{(\omega_j(\mathbf{p}) + \omega_\ell(\mathbf{p}))^3}. \quad (59)$$

The results (34) and (58) show that both Ξ and the diagonal elements \mathcal{Q}_{11} and \mathcal{Q}_{22} are logarithmically divergent (of order $\ln \Lambda/M$ or $\ln \Lambda/\Delta$), while the off-diagonal elements \mathcal{Q}_{12} are finite. In the following, we drop the finite off-diagonal terms, following the standard prescription of considering only the ultraviolet-divergent pieces up to logarithmic accuracy of the bubble diagrams in effective bosonized theories (see e.g., [39–41]). The dropped \mathcal{Q}_{12} terms would result in anomalous crossing terms $\sim \partial_\mu \hat{\theta}_\pi \partial^\mu \hat{\theta}_d$ which are absent in general parametrizations of pionic mode kinetic energies (up to second order in the pionic fields) in the literature, e.g., [12]. After this procedure, we identify the remaining diagonal elements of \mathcal{Q} as the squared decay constants for the vacuum pion and the diquark-condensate pion:

$$f_\pi^2 = \mathcal{Q}_{11}, \quad f_{\tilde{\pi}}^2 = \mathcal{Q}_{22}; \quad (60)$$

that is, $\mathcal{Q} = \mathcal{F}^2 = \text{diag}(f_\pi^2, f_{\tilde{\pi}}^2)$, where $\mathcal{F} = \text{diag}(f_\pi, f_{\tilde{\pi}})$ as in Eq. (37). Similarly dropping the finite off-diagonal

terms of the velocity matrix \mathcal{Q}_v , we obtain $\mathcal{Q}_v = \text{diag}(v_\pi^2, v_{\tilde{\pi}}^2) \mathcal{Q}$, where the velocities are

$$\begin{aligned} v_\pi^2 &= \mathcal{Q}_{v11} = f_\pi^{-2} \frac{\partial B_{\pi\pi}(0)}{\partial \mathbf{k}^2}, \\ v_{\tilde{\pi}}^2 &= \mathcal{Q}_{v22} = f_{\tilde{\pi}}^{-2} \frac{\partial B_{dd}(0)}{\partial \mathbf{k}^2}. \end{aligned} \quad (61)$$

In terms of the pion fields $\pi(x) = f_\pi \hat{\theta}_\pi(x)$ and $\tilde{\pi}(x) = f_{\tilde{\pi}} \hat{\theta}_d(x)$, the effective Lagrangian density is now

$$\begin{aligned} &\frac{1}{2} \vec{\theta}^T \left(-\mathcal{Q} \partial_t^2 + \mathcal{Q}_v \vec{\partial}^2 - \Xi \right) \vec{\theta} \\ &\equiv \frac{1}{2} \vec{\pi}^T (-\partial_t^2 + \text{diag}(v_\pi^2, v_{\tilde{\pi}}^2) \vec{\partial}^2 - \Sigma) \vec{\pi}, \end{aligned} \quad (62)$$

where $\vec{\pi}(x) \equiv (\pi(x), \tilde{\pi}(x))^T = \mathcal{F} \vec{\theta}(x)$. The inverse propagator in Eq. (62) is again diagonalized by Eq. (38), in terms of the NG mode π_G and the massive mode π_M . Furthermore, in terms of $\hat{\theta}_\pi$ and $\hat{\theta}_d$, we write

$$\pi_G = \frac{f_\pi^2 \hat{\theta}_\pi + f_{\tilde{\pi}}^2 \hat{\theta}_d}{\sqrt{f_\pi^2 + f_{\tilde{\pi}}^2}} \equiv f_G \hat{\theta}_G \quad (63)$$

where $\hat{\theta}_G$, the chiral NG boson degree of freedom, is the fluctuation corresponding to the universal axial $U(1)_A$ rotation of the whole system from the scalar state; such rotation corresponds to the simultaneous rotation of $\hat{\theta}_\pi$ and $\hat{\theta}_d$, therefore $\hat{\theta}_G = \hat{\theta}_\pi = \hat{\theta}_d$. As a result,

$$f_G^2 = f_\pi^2 + f_{\tilde{\pi}}^2, \quad (64)$$

thus relating the decay constant of the NG boson f_G to the decay constants f_π and $f_{\tilde{\pi}}$ for the corresponding chiral rotations of the $\langle \bar{q}q \rangle$ and $\langle q\bar{q} \rangle$ order parameters. As Eq. (63) shows f_π^2 and $f_{\tilde{\pi}}^2$ can be understood as the “weight functions” of π and $\tilde{\pi}$ within the NG mode π_G .

The plot of f_G , f_π and $f_{\tilde{\pi}}$ as functions of quark density in Fig. 5 shows that the decay constant of the NG pion, f_G , always increases with increasing quark density, whereas f_π decreases with density; the behavior of f_π is in agreement with the prediction of in-medium chiral perturbation theory [42] that to leading order in the density the pion decay constant decreases from its vacuum value linearly.⁸ The different behavior of f_G and f_π arises from the presence of diquark pairing at all densities in our schematic model; even at low density, the BCS gap causes f_G to increase with increasing density despite $\langle \bar{q}q \rangle$ (and thus f_π) gradually shrinking at the same time.⁹

⁸ Unlike NJL discussions of quark matter, reference [42] discusses only a nucleon medium. Although the vacuum cannot be described by deconfined NJL quark matter, the behavior of its chiral NG mode under modification of the density does connect qualitatively well with such nuclear matter models, a similarity suggesting that the transition from nuclear matter to high density quark matter could have continuous dynamic chiral symmetry breaking.

⁹ Realistically, the homogeneous diquark pairing described in the present model does not appear in the low density QCD phase diagram, owing to the onset of confinement.

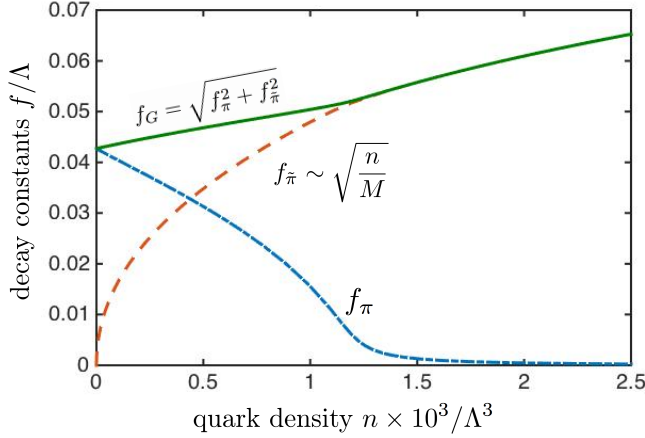


Figure 5. (Color online) Decay constants f_G , f_π and $f_{\tilde{\pi}}$ as functions of quark density n , with $G = 11\Lambda^{-2}$ and $H = 6\Lambda^{-2}$.

The low density behavior of $f_{\tilde{\pi}}$ and Δ can be derived from the pairing gap equation (19) and the bubble results Eq. (58). Isolating the divergent part $1/\omega_+$ in the gap equation integral, one can show that in the limit $n \rightarrow 0$, the gap behaves like

$$\frac{\Delta}{\Lambda} \sim \frac{p_F}{M} e^{-\pi^2/HMp_F}, \quad (65)$$

indicating that Δ/n goes to 0 as n goes to 0. Similarly, by isolating the divergent piece of the bubble integral in Eq. (58) in the $(j, \ell) = (+, +)$ part of the sum, one can show that in the limit $n \rightarrow 0$, $f_{\tilde{\pi}} \sim \sqrt{n/M}$, and $\Delta^2/f_{\tilde{\pi}}^2 \sim \Delta^2 M/n \rightarrow 0$.

The decay constant f_G can be equivalently parametrized as the vector transition amplitude from a state with one generalized pion to the vacuum via the time component of the axial current $J_A^\mu \equiv \bar{\psi} i \gamma^\mu \gamma^5 \psi / 2$, in the same way as in the vacuum pion treatment [24] in NJL models:

$$\begin{aligned} i f_G k^0 &= \langle 0 | J_A^0 | \pi_G \rangle = \frac{1}{f_G} \langle 0 | J_A^0 | f_\pi \pi + f_{\tilde{\pi}} \tilde{\pi} \rangle \\ &= \frac{1}{f_G} i (f_\pi^2 + f_{\tilde{\pi}}^2) k^0, \end{aligned} \quad (66)$$

again confirming Eq. (64).

The density-dependent Nambu-Gor'kov interaction vertices coupling π_G and π_M to the Nambu-Gor'kov quark field ψ can also be written in terms of the decay constants. Using the perturbed quark inverse propagator with the bosonized fields in Eqs. (42) and (43), and the transformation Eq. (38), we write the bosonized interaction as

$$\begin{aligned} \mathcal{L}_{\text{int}} &= \bar{\psi} \left(\frac{M}{f_\pi} \Gamma_\pi \pi + \frac{\Delta}{f_{\tilde{\pi}}} \Gamma_{\tilde{\pi}} \tilde{\pi} \right) \psi \\ &= \bar{\psi} (\Gamma_G \pi_G + \Gamma_M \pi_M) \psi, \end{aligned} \quad (67)$$

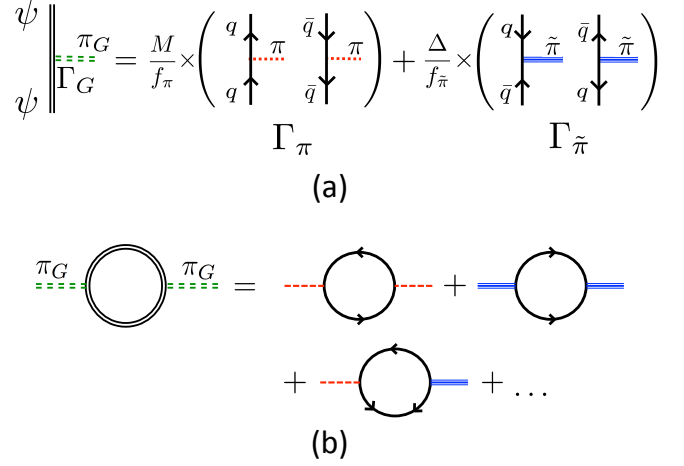


Figure 6. (Color online) (a) Diagrammatic decomposition of quark- π_G coupling Γ_G into chiral Γ_π and diquark $\Gamma_{\tilde{\pi}}$ vertices. The (green) dashed double line represents the π_G field. The Nambu-Gor'kov field ψ (black, double line) contains both the quark and charge-conjugate quark fields, thus including the quark field (black, solid, arrowed line) propagating in either time direction; Γ_π is the coupling matrix between vacuum pion π (red, dashed line) and the pseudoscalar $\bar{q}q$ quark sector, and $\Gamma_{\tilde{\pi}}$ is the coupling matrix between vacuum pion $\tilde{\pi}$ (blue, double line) and the pseudoscalar qq sector. (b) Characteristic bubble diagrams contributing to the resulting self-energy of π_G in the Nambu-Gor'kov formalism, including both direct bubbles, $B_{\pi\pi}$ and B_{dd} , and mixing bubbles, $B_{\pi d}$.

where the interaction vertices,

$$\begin{aligned} \Gamma_G(\mu) &\equiv \frac{1}{f_G} (M \Gamma_\pi + \Delta \Gamma_{\tilde{\pi}}), \\ \Gamma_M(\mu) &\equiv \frac{1}{f_G} \left(\frac{f_{\tilde{\pi}}}{f_\pi} M \Gamma_\pi - \frac{f_\pi}{f_{\tilde{\pi}}} \Delta \Gamma_{\tilde{\pi}} \right), \end{aligned} \quad (68)$$

are matrix functions of μ , describing the coupling of π_G and π_M to the chiral $\bar{q}q$ and diquark pairing qq sectors of the quark medium. Figure 6 represents the diagrammatical representation of the decomposition of Γ_G . The coupling strengths to the chiral sector and the diquark sector are given by the weightings M/f_G and Δ/f_G ; in the vacuum limit $\Delta/f_G = 0$, and the former simply reduces to g_π , the residue of the pion pole in the $\bar{q}q$ - qq scattering T-matrix, related to M and f_π via the familiar Goldberger-Treiman relation $g_\pi = M/f_\pi$.

In more realistic NJL models with multiple flavors present, possible asymmetric chiral and diquark pairings due to the heavy strange quark, and the Kobayashi-Maskawa-'t Hooft six-quark instanton interaction [43–45] provide additional $\bar{q}q$ - qq mixing, with further modifications of Γ_G and Γ_M . We leave this topic to a future publication.

D. Finite bare quark mass $m_q \neq 0$

We now turn on a finite but small bare quark mass m_q , explicitly breaking the chiral symmetry, to investigate its effect on the mass matrix Σ . We obtain the perturbed Σ by directly taking second order derivatives of Ω with respect to θ_π and θ_d , using Eq. (8).

We first review the familiar σ - π sector alone, where there is only one mode π present. As seen from the quasiparticle spectrum, $\omega_\pm(\mathbf{p})$, Eq. (6), m_q slightly shifts σ , causing the system to favor a negative value for σ (whence the sign in the parametrization $\sigma = -M \cos \theta_\pi$). In the vacuum scalar state, the eigenvalues expanded to leading order in m_q are :

$$\begin{aligned} \omega_\pm(\mathbf{p}) &= \left| \pm (\mathbf{p}^2 + m_q^2 + \sigma^2 + \pi^2 - 2m_q\sigma)^{1/2} - \mu \right| \\ &= \omega_\pm(\mathbf{p})_{m_q=0} \\ &\quad + \left(\pm \frac{\mu}{\sqrt{\mathbf{p}^2 + \sigma^2 + \pi^2}} - 1 \right) \frac{\sigma m_q}{\omega_\pm(\mathbf{p})_{m_q=0}}. \end{aligned} \quad (69)$$

As a result, the free energy becomes

$$\begin{aligned} \Omega &= \Omega_{m_q=0} + \sigma m_q \sum_\pm \int_{\mathbf{p}} \frac{1}{\omega_\pm} \left(1 \mp \frac{\mu}{\sqrt{\mathbf{p}^2 + \sigma^2 + \pi^2}} \right) \\ &\approx \Omega_{m_q=0} + \frac{\sigma m_q}{2G}, \end{aligned} \quad (70)$$

where we have used the gap equation Eq. (18) in writing the second line, up to linear order in m_q . With the parametrization (26), this term effectively adds a positive stiffness term for $\theta_\pi^2 \sim \pi^2$, since $\sigma = -M(1 - \theta_\pi^2/2 + \dots)$. We thus retrieve the GMOR result for the vacuum pion mass,

$$f_\pi^2 m_\pi^2 = \frac{M}{2G} m_q = -\langle \bar{q}q \rangle m_q, \quad (71)$$

to leading order linear in m_q .

We also consider the pure BCS limit without the chiral σ - π sector, setting $M = 0$, and assuming zero phase difference ϕ between Δ_s and Δ_{ps} . The quasiparticle spectrum becomes

$$\omega_\pm^2(\mathbf{p}) = \mathbf{p}^2 + \mu^2 + \Delta^2 \mp 2\sqrt{(|\mathbf{p}|\mu)^2 + m_q^2 |\Delta_{ps}|^2}. \quad (72)$$

The pseudoscalar diquark NG mode $\tilde{\pi}^2 \sim \theta_d^2 \sim |\Delta_{ps}|^2$ picks up a mass, given by

$$f_\pi^2 m_\pi^2 = a \Delta^2 m_q^2, \quad (73)$$

as one sees from the leading order correction to Ω , of order m_q^2 , instead of m_q for the π :

$$\Omega = \Omega_{m_q=0} + \frac{1}{2} a m_q^2 |\Delta_{ps}|^2 + \mathcal{O}(m_q^4). \quad (74)$$

Unlike in the σ - π sector, the diquark mean fields Δ_s and Δ_{ps} are neither coupled directly nor offset by m_q

at the level of the mean field Lagrangian; instead, the diquark fields indirectly couple to m_q via the mixing term $|(m_q - \sigma)\Delta_{ps} - \pi\Delta_s|^2$. This term is the key to generating the mass of the NG mode in the BCS phase.

The difference in the leading order dependence on m_q of the GMOR relations in the vacuum phase and the high density BCS phase, which is also present in the more realistic $N_f = 3$, $N_c = 3$ case, can be understood as originating from the $U(1)_A$ axial symmetry. Specifically, when one writes down a general Ginzburg-Landau effective Lagrangian in terms of the chiral and diquark condensates, the term of lowest non-zero order in m_q and the diquark condensates that respects $U(1)_A$ symmetry is of order m_q^2 [9, 12]. As a result, at high density, where diquark pairing dominates, the chiral NG bosons should obey a GMOR relation $\sim m_q^2$. A subtle complication in more realistic models is that the axial $U(1)_A$ symmetry is explicitly broken by quantum effects (the axial anomaly) at lower densities, which permits an additional mass term for the diquark condensates of order m_q . In this case, the chiral NG bosons might still obey a GMOR relation $\sim m_q$ in leading order even with dominating diquark condensates at moderate densities. Nevertheless, it is known that at high density the axial anomaly is heavily suppressed [46, 47] greatly reducing such a $U(1)_A$ -violating term; the GMOR relation is then restored to $\sim m_q^2$ in leading order.¹⁰

Finally we calculate the perturbed mass of π_G and π_M , in the intermediate density coexistence phase. The two limits considered above – the pure σ - π sector limit and the pure BCS limit – indicate that we must keep effects of m_q up to second order, and allow fluctuations in both π and Δ_{ps} – achieved by small fluctuations of $\vec{\theta} = (\theta_\pi, \theta_d)^T$. Expanding Ω in terms of $\vec{\theta}$ up to second order, we find

$$\Omega(\theta_\pi, \theta_d) = \Omega(0, 0) + \frac{1}{2} \vec{\theta}^T \Xi(m_q) \vec{\theta} + \dots, \quad (75)$$

where (cf. Eq. (34))

$$\Xi(m_q) = \begin{pmatrix} bMm_q + aM^2\Delta^2 & -aM\Delta^2(M + m_q) \\ -aM\Delta^2(M + m_q) & a(M + m_q)^2\Delta^2 \end{pmatrix}; \quad (76)$$

here

$$b = \int_{\mathbf{p}} \sum_\pm \frac{1}{\omega_\pm} \left(1 - \frac{\mu}{\epsilon_\pm} \right), \quad (77)$$

the integral on the right side of the gap equation (18), is a function of M , Δ , μ , and m_q . In the chiral limit $m_q = 0$

¹⁰ Diquark pairing is not the only known mechanism that can modify the meson mass GMOR relation. The asymmetry in quark flavors could have a similar effect of inducing higher order GMOR relations, such as pions in an isospin-asymmetric medium [48, 49].

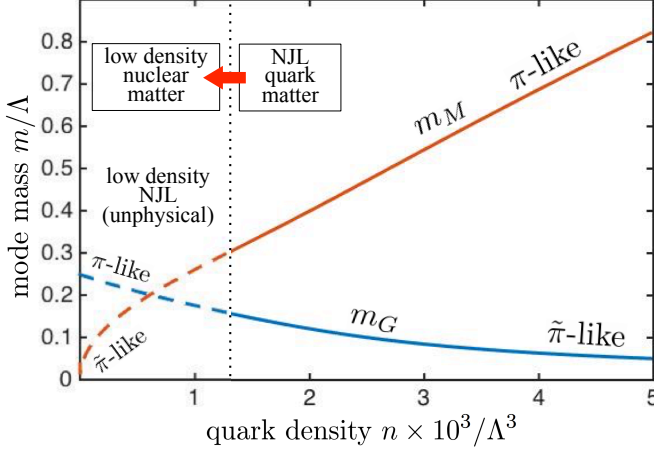


Figure 7. The perturbed masses of the NG mode, m_G , and of the heavy mode, m_M , as functions of quark density, n . Here we take $G = 11\Lambda^{-2}$, $H = 6\Lambda^{-2}$ and $m_q = 0.01\Lambda$. With decreasing density, m_M rapidly decreases as the Fermi surface vanishes, eventually crossing the NG-mode mass m_G ; this is an artifact of our simplified NJL model which does not take confinement into account. Realistically this low density regime is instead described by nuclear matter; the boundary of the transition from quark matter to nuclear matter drawn in the plot is only illustrative.

in the chirally broken phase with $M \neq 0$, b reduces to $1/2G$. In terms of the mass matrix $\Sigma = \mathcal{F}^{-1}\Xi\mathcal{F}^{-1}$ for the pion fields $\vec{\pi}$, we obtain the following matrix generalization of the GMOR relation encompassing both modes:

$$\begin{aligned} \mathcal{F}\Sigma\mathcal{F} &= M^2 a \Delta^2 \begin{pmatrix} 1 & -1 \\ -1 & 1 \end{pmatrix} + M m_q \begin{pmatrix} b & -a\Delta^2 \\ -a\Delta^2 & 2a\Delta^2 \end{pmatrix} \\ &\quad + a\Delta^2 m_q^2 \begin{pmatrix} 0 & 0 \\ 0 & 1 \end{pmatrix} \\ &\equiv \Xi + M m_q \Xi_I + a\Delta^2 m_q^2 \Xi_{II}. \end{aligned} \quad (78)$$

Equation (78) can be readily generalized to systems with more complex chiral order parameters than $\langle \bar{q}q \rangle$ and $\langle qq \rangle$. Despite appearances Eq. (78) is not actually a series expansion in m_q , since a , b , f_π , $f_{\tilde{\pi}}$, Δ and M are themselves functions of m_q .

The structure of Eq. (78) clearly reflects the underlying physics. The leading term Ξ is a consequence of Goldstone's theorem, as argued before. The perturbations to the stiffness matrix $\delta\Xi \equiv M m_q \Xi_I + a\Delta^2 m_q^2 \Xi_{II}$ contain combinations of order parameters that violate the $U(1)_A$ chiral symmetry, such as $\sigma|\Delta_s|^2$ and σ ; they are results of m_q explicitly breaking chiral symmetry.

For non-zero m_q , to leading order in $\delta\Xi$ the perturbed

squared masses are given by

$$\begin{aligned} m_G^2 &\approx \frac{bMm_q + a\Delta^2 m_q^2}{f_G^2}, \\ m_M^2 &\approx aM^2 \Delta^2 \left(\frac{1}{f_\pi^2} + \frac{1}{f_{\tilde{\pi}}^2} \right) + Mm_q \left(\frac{bf_{\tilde{\pi}}^2}{f_G^2 f_\pi^2} + \frac{2a\Delta^2}{f_\pi^2} \right) \\ &\quad + m_q^2 \frac{a\Delta^2 f_\pi^2}{f_G^2 f_\pi^2}. \end{aligned} \quad (79)$$

Figure 7 shows m_G and m_M as functions of the quark density n . In the relatively high density BCS regime, m_G decreases with increasing density as a consequence of the increasing BCS pairing $\langle qq \rangle$ taking on the role of chiral order parameter; $f_{\tilde{\pi}}$ increases while f_π vanishes. From the mixing, Eq. (38), one sees that the π_G mode is mainly composed of $\tilde{\pi}$ -like fluctuations, while the massive mode is mainly π -like, being heavy due to vanishing $\langle \bar{q}q \rangle$. The NG-mode mass obeys the diquark-condensate pion GMOR relation (cf. Eq. (73)):

$$f_G^2 m_G^2 \approx a m_q^2 \Delta^2. \quad (80)$$

At low density, the π_G mode is primarily π -like, and one recovers the vacuum pion GMOR relation (cf. Eq. (71)):

$$f_G^2 m_G^2 \approx bMm_q \approx \frac{Mm_q}{2G} \approx -\langle \bar{q}q \rangle m_q \quad (81)$$

to leading order in m_q .

On the other hand, since the heavy mode π_M is $\tilde{\pi}$ -like at low density, m_M vanishes in the limit $n \rightarrow 0$, crossing with m_G in the process. Such behavior is an artifact of the present schematic model: since diquark pairing is present at arbitrarily low densities in the model, the $\tilde{\pi}$ -like mode, corresponding to chiral fluctuations of pairing amplitude $\langle qq \rangle$ mainly near the Fermi surface, the free energy cost goes to zero as the Fermi surface vanishes. In the vacuum this mode is simply not present.

The density at which m_M crosses m_G can be roughly estimated using Eq. (79) and the fact that $\Delta \ll f_{\tilde{\pi}}$ at low density (see Eq. (65) and its comments) to show that when $m_G \sim m_M$, the decay constants are comparable with each other: $f_\pi \sim f_{\tilde{\pi}}$. Since $f_{\tilde{\pi}}^2 \sim n/M$ at low density, $f_\pi \sim f_{\tilde{\pi}}$ implies $n \sim f_\pi^2 M$, a characteristic density scale for chiral symmetry breaking via $\langle \bar{q}q \rangle$. Using values from realistic NJL models where the effective quark mass M is ~ 300 MeV and the experimental f_π is ~ 92 MeV, we find that n is of order nuclear matter density, $n_0 \approx 0.16 \text{ fm}^{-3}$. In this density regime, QCD confinement binds quarks into nucleons, and the homogeneous diquark pairing picture in the schematic model at these densities is no longer physical. Nevertheless, the π_G mode does obey the well-known vacuum pion GMOR relation in the low density limit, allowing this pionic mode to be smoothly interpolated between nuclear matter and quark matter at high density, where chiral symmetry remains broken throughout.

VI. OUTLOOK

Having elaborated the construction and the density-dependent behavior of the generalized pion π_G , we briefly discuss several implications of the results obtained so far, and open questions for future research.

1. *Bose-Einstein condensation of the generalized pion π_G .* The existence of the light π_G mode at all densities, as detailed in Sec. V, raises the interesting possibility of the modes becoming Bose condensed. Homogeneous condensates of the pionic NG modes have been considered, within NJL, in both the low density non-BCS (e.g., [50]) and high density BCS (e.g., [51]) limits. In the present schematic model however, such condensation is trivial, since it merely corresponds to a global axial $U(1)_A$ rotation of the system from the scalar state. In the chiral limit, the chiral symmetry is respected by the Lagrangian, and such rotation does not cost any free energy; the rotated system is energetically equivalent to the original scalar state. With a finite m_q breaking chiral symmetry, the scalar state is the unique ground state with the lowest free energy, since there are no forces driving condensation, and homogeneous pion condensates are unstable.

In more realistic NJL models, however, where multiple flavors and charge neutrality are taken into account, several factors driving pionic condensation emerge. For example, the mismatched Fermi surfaces of up and down quarks and an electric charge chemical potential translate directly into an effective chemical potential of the charged pions (see discussions of pion condensation in NJL models in [17, 52–58]). When the effective pion chemical potential overwhelms the pion mass, even homogeneous pion condensation can occur. Furthermore, as the pions directly couple to the quarks in the pseudoscalar $\bar{q}q$ and qq channels as discussed in Sec. V C, more types of pionic condensates could be favored by the pion interacting with the quark matter medium at different densities, such as inhomogeneous meson condensates (e.g., [59, 60]) or condensation into states with finite momenta. Other exotic phases involving inhomogeneous chiral or diquark condensates (e.g., [61, 62]) could also affect pion condensation. We will discuss these possibilities in a future publication.

2. *Generalized meson mass ordering reversal.* Reproducing the mass ordering reversal phenomenon as discussed in Ref. [9] again requires generalizing the present schematic model to three flavors and colors, with the strange quark heavier than the up and down quarks, and allowing for asymmetric pairing between the three flavors and colors due to mismatched Fermi surfaces at intermediate density. The masses and decay constants of the generalized meson octet as functions of density

can then be computed in the same way to study the the density-dependent meson mass spectrum throughout different phases, and how those mass curves depend on model parameters. Such an analysis is required for further study of generalized meson condensation in realistic quark matter.

3. *Connection to nuclear matter pions.* The interaction between vacuum pion mode π and the quarks are the same as the nucleon-pion interaction in sigma model. When diquark pairing is taken into account, the pion-quark interaction is modified into the density-dependent generalized Γ_G vertex, which significantly reduces the generalized pion mass at higher density (see Fig. 7). It is thus natural to ask whether nucleon-nucleon pairing at relatively high density (but still within the nuclear matter regime) would result in a similar modification to the generalized pion properties; as a consequence a one-to-one mapping between chirally broken nuclear matter to chirally broken quark matter in terms of generalized pions may be formed. Such a continuity in chiral symmetry breaking would provide further insight into possible continuity between nuclear matter and quark matter.

4. *Possible role of the $\hat{\phi}$ mode.* This mode, discussed in Sec. V, could also play a role in a realistic phase diagram (a possibility that has not received attention in present NJL studies). Although the $\hat{\phi}$ mode, not being a NG mode, is always massive, there may be density regions where its mass is significantly reduced. This observation comes from the fact that the $\hat{\phi}$ mode corresponds to a relative phase oscillation between the scalar diquark condensate Δ_s and the pseudoscalar Δ_{ps} . Specifically, its stiffness term,

$$\frac{\partial^2 \Omega}{\partial \sin^2 \phi} = \frac{\Delta^4}{16} \sin^2 2\theta_d \sum_{\pm} \int_{\mathbf{p}} \frac{1}{\omega_{\pm}^3} > 0, \quad (82)$$

(calculated here, for simplicity, in the pure BCS limit with a finite θ_d chiral rotation from the scalar state in our model) can be made small if either the BCS gap Δ or the (homogeneous generalized pion condensation) θ_d is small. The possible role of the ϕ mode in the low energy physics of dense quark matter and its coupling to the pseudoscalar Δ_{ps} fluctuations and thus its coupling to the generalized pion will be explored in a future study as well.

ACKNOWLEDGMENTS

We are grateful to Tetsuo Hatsuda for his careful critique of this paper. This research was supported in part by NSF Grant PHY1305891.

[1] M. Alford, A. Schmitt, K. Rajagopal and T. Schäfer, Rev. Mod. Phys. **80**, 4, 1455 (2008), and references therein.

[2] S. B. Rüster, V. Werth, M. Buballa, I. A. Shovkovy, and D. H. Rischke, Phys. Rev. D **72**, 034004 (2005).

- [3] D. Blaschke, S. Fredriksson, H. Grigorian, A. M. Öztaş, and F. Sandin, Phys. Rev. D **72**, 065020 (2005).
- [4] D. Müller, M. Buballa, and J. Wambach, J. Eur. Phys. J. A **49**: 96 (2013).
- [5] K. Fukushima and T. Hatsuda, Rep. Prog. Phys. **74**, 014001 (2011).
- [6] S. Muroya, A. Nakamura, C. Nonaka, and T. Takaishi, Prog. Theor. Phys. **110**, 615 (2003).
- [7] M. Alford, K. Rajagopal and F. Wilczek, Nucl. Phys. B **537**, 443 (1999).
- [8] R. D. Pisarski and D. H. Rischke, Proc. of the Judah Eisenberg Memorial Symposium, Tel Aviv, April 14 - 16; arXiv:nucl-th/9907094 (1999).
- [9] D. T. Son and M. A. Stephanov, Phys. Rev. D **61**, 074012 (2000).
- [10] K. Fukushima, Phys. Rev. D **70**, 094014 (2004).
- [11] M. Rho, A. Wirzba, and I. Zahed, Phys. Lett. B **473**, 126 (2000).
- [12] N. Yamamoto, M. Tachibana, T. Hatsuda and G. Baym, Phys. Rev. D **76**, 074001 (2007).
- [13] T. Kojo, Phys. Lett. B **769** 14 (2016).
- [14] V. Bernard, Phys. Rev. D **34**, 5 (1986).
- [15] D. Ebert, T. Feldmann, R. Friedrich, and H. Reinhardt, Nucl. Phys. B **434**, 619 (1995).
- [16] M. Oertel, M. Buballa, and J. Wambach, Nucl. Phys. A **676**, 247 (2000).
- [17] L. He, M. Jin, and P. Zhuang, Phys. Rev. D **71**, 116001 (2005).
- [18] H. Hansen, W. M. Alberico, A. Beraudo, A. Molinari, M. Nardi, and C. Ratti, Phys. Rev. D **75**, 065004 (2007).
- [19] V. Kleinhaus, M. Buballa, D. Nickel, and M. Oertel, Phys. Rev. D **76**, 074024 (2007).
- [20] M. Ruggieri, JHEP 0707, 031 (2007).
- [21] D. Ebert, K.G. Klimenko, and V.L. Yudichev, Eur. Phys. J. C **53**, 65 (2008).
- [22] Y. Nambu and G. Jona-Lasinio, Phys. Rev. **122**, 345 (1961).
- [23] Y. Nambu and G. Jona-Lasinio, Phys. Rev. **124**, 246 (1961).
- [24] M. Buballa, Phys.Rept. **407**, 205 (2005).
- [25] T. M. Schwarz, S. P. Klevansky, and G. Papp, Phys. Rev. C **60**, 055205 (1999).
- [26] T. Hatsuda and T. Kunihiro, Phys. Rep. **247**, 22 (1994).
- [27] K. Fukushima, Phys. Letters B **591**, 277 (2004).
- [28] H. J. Warringa and D. Boer, Phys. Rev. D **72**, 014015 (2005).
- [29] C. Ratti, M. A. Thaler, and W. Weise, Phys. Rev. D **73**, 014019 (2006).
- [30] S. Röckner, C. Ratti, and W. Weise, Phys. Rev. D **75**, 034007 (2007).
- [31] H. Abuki, Prog Theor Phys **174**: 66 (2008).
- [32] H. Abuki, G. Baym, T. Hatsuda, and N. Yamamoto, Phys. Rev. D **81**, 125010 (2010).
- [33] G. Y. Shao, M. Di Toro, V. Greco, M. Colonna, S. Plumari, B. Liu and Y. X. Liu, Phys. Rev. D **84** 3, 034028, (2011).
- [34] P. D. Powell and G. Baym, Phys. Rev. D **85**, 074003 (2012).
- [35] P. D. Powell and G. Baym, Phys. Rev. D **88**, 014012 (2013).
- [36] P. D. Powell, Doctoral dissertation, University of Illinois at Urbana-Champaign, 2013.
- [37] D. G. Yakovlev, A.D. Kaminker, O.Y. Gnedin, and P. Haensel, Phys. Rep. **354**, 1(2001).
- [38] N. Bilić, K. Demeterfi and B. Petersson, Nucl. Phys. B **377**, 651 (1992).
- [39] T. Eguchi, Phys. Rev. D **14**, 2755 (1976).
- [40] M. K. Volkov, Ann. Phys. **157**, 282 (1984).
- [41] D. Ebert and M. K. Volkov, Z. Phys. C. Particles and Fields **16**, 205 (1983).
- [42] S. Goda and D. Jido, Prog. Theor. Exp. Phys. 033D03 (2014).
- [43] M. Kobayashi and T. Maskawa, Prog. Theor. Phys. **44**, 1422 (1970).
- [44] G. 't Hooft, Phys. Rev. Lett. **37**, 8 (1976).
- [45] G. 't Hooft, Phys. Rep. **142**, 357 (1986).
- [46] R. Rapp, T. Schäfer, E. V. Shuryak, and M. Velkovsky, Ann. Phys. (N.Y.) **280**, 35 (2000).
- [47] T. Schäfer, Phys. Rev. D **65**, 094033 (2002).
- [48] T. D. Cohen and W. Broniowski, Phys. Lett. B **348** 12 (1995).
- [49] W. Broniowski and B. Hiller, Phys. Lett. **392** 267 (1997).
- [50] J. Anderson and L. Kyllingstad, J. Phys. G: Nucl. Part. Phys. **37** 015003 (2010).
- [51] M. Buballa, Phys. Lett. B **609**, 57 (2005).
- [52] P.F. Bedaque and T. Schäfer, Nucl. Phys. A **697**, 802 (2002).
- [53] D. Ebert and K. G. Klimenko, J. Phys. G: Nucl. Part. Phys. **32**, 599 (2006).
- [54] D. Ebert and K. G. Klimenko, Eur. Phys. J. C **46**: 771 (2006).
- [55] X. Hao and P. Zhuang, Phys. Lett. B **652**, 275 (2007).
- [56] H. Abuki, M. Ciminale, R. Gatto, N. D. Ippolito, G. Nardulli and M. Ruggieri, Phys. Rev. D **78**, 014002 (2008).
- [57] H. Abuki, R. Anglani, R. Gatto, M. Pellicoro, and M. Ruggieri, Phys. Rev. D **79**, 034032 (2009).
- [58] J. O. Andersen and L. T. Kyllingstad, J. Phys. G: Nucl. and Part. Phys. **37**, 015003 (2010).
- [59] M. M. Forbes, Phys. Rev. D **72**, 094032 (2005).
- [60] N. V. Gubina, K. G. Klimenko, S. G. Kurbanov, and V. Ch. Zhukovsky, Phys. Rev. D **86**, 085011 (2012).
- [61] M. Buballa and S. Carignano, Prog. Part. Nucl. Phys **81**, 39 (2015).
- [62] M. Alford, J. A. Bowers and K. Rajagopal, Phys. Rev. D **63**, 074016 (2001).